

## Measurement of the Sea Surface Emissivity

MASANORI KONDA<sup>1</sup>, NORIHISA IMASATO<sup>1</sup>, KATSUYA NISHI<sup>1</sup> and TAKASHI TODA<sup>2</sup>

<sup>1</sup>*Department of Geophysics, Kyoto University, Kyoto 606, Japan*

<sup>2</sup>*Lake Biwa Museum Project Office, Shiga Prefecture Board of Education, Otsu 520, Japan*

(Received 14 May 1993; in revised form 26 July 1993; accepted 28 July 1993)

**The sea surface emissivity in the infrared region is determined on the basis of data analyses. Net radiation, surface irradiance and other oceanographical and meteorological variables are measured throughout most of the year at the oceanographical observatory tower in Tanabe Bay, Japan. We have found that  $0.984 \pm 0.004$  is a reliable emissivity value from the night time data. Surface emission radiates not from the subsurface water but from the sea surface. The thermal skin layer on the sea surface, however, is disturbed and disappears under high wind speed over 5 m/s through the analyses of the radiation observation using the emissivity value of 0.984. Under low wind speed, the sea surface can be cooler or warmer than the subsurface due to overlying thermal conditions, and the skin layer can be neutral as the transient process between them. By using an emissivity value of 0.984, the temperature difference between the sea surface temperature and the temperature determined from surface irradiance that has been reported in the satellite data analyses is found to be reduced by half.**

### 1. Introduction

Recently, satellite infrared observations and the sea surface temperature (SST) image from space are often used in various studies. To apply satellite image data in quantitative studies, the temperature retrieval methodology should be improved to obtain a more accurate SST.

A difficulty in obtaining a highly accurate SST stems from the atmospheric attenuation correction. Though many studies have been performed by assuming the sea surface as a blackbody, the sea surface is actually a graybody and it is necessary to determine the value of emissivity.

There are two major problems with the attempt of previous studies to determine the value of emissivity. First, when the infrared surface emissivity of the ocean is less than 1.00, reflection at the surface should be considered. Total radiation from the sea surface into the bottom of the atmosphere is the sum of the surface radiation and the reflection of atmospheric radiation at the surface. Therefore, when we observe surface irradiance, we should separate the surface emission from the surface reflection. Second, the temperature differences across the cool skin on the sea surface should be considered. Cool skin is conventionally considered to lie in the upper few centimeters or millimeters of the ocean (Woodcock, 1941; Hasse, 1963; McAlister and McLeish, 1969; Paulson and Simpson, 1981; etc.). However, there are no field measurements to directly determine the thickness of the surface skin layer (Katsaros, 1980). The temperature difference  $\Delta T$  between the ocean-air interface and an ocean depth of some tens of centimeters is, according to Saunders (1967a), proportional to  $\nu Q/\kappa U_*$ . Here  $\nu$  is the kinetic viscosity of water,  $\kappa$  the thermal conductivity,  $U_*$  the friction velocity, and  $Q$  the heat flux. Schluessel *et al.* (1990) asserts that  $\Delta T$  is about  $0.2^\circ\text{C}$  on average and varies between  $1.0^\circ\text{C}$  and  $-1.0^\circ\text{C}$ . Because of the thinness

Table 1. The summary of the former emissivity studies.

Emissivity	Study	Summary of the method
0.993	Buettner and Kern (1965)	not considering the skin layer
0.986	Saunders (1967b, 1968)	observation of the reflectance from the air plane
0.9875	Mikhaylov and Zolotarev (1970)	calculation from the optical constant
0.992 (11 $\mu\text{m}$ )	Masuda <i>et al.</i> (1988)	calculation of the reflectance using the numerical model surface
0.972	Davies <i>et al.</i> (1971)	observation of sheltered watersurface from the sky

of the cool skin, it is almost impossible to directly observe the surface skin temperature,  $T_s$ , whereas it is possible to observe the subsurface temperature.

Buettner and Kern (1965) estimated the sea surface emissivity to be 0.993 from an experiment using an emissivity box, but they disregarded the temperature difference across the cool skin. Saunders (1967b, 1968) observed the plane sea surface irradiance from an airplane and determined the reflectance. By determining the reflectance as the ratio of the differences in energy between the clear and the cloudy sky at different places, he calculated the emissivity to be 0.986. The process of separating the reflection from the surface irradiance, however, is not precise. Mikhaylov and Zolotarev (1970) calculated the emissivity from the optical constant of the water and found the average in the infrared region was 0.9875. The observation of Davies *et al.* (1971) was performed on Lake Ontario with a wave height less than 25 cm. They measured the surface emission isolated from sky radiation by an aluminum cone, and estimated the emissivity to be 0.972. The aluminum was assumed to act as a mirror in infrared region. In fact, aluminum does not work as a perfect mirror. Masuda *et al.* (1988) computed the surface emissivity as a function of the zenith angle of observed radiation and wind speed. They computed the emissivity from the reflectance of a model sea surface consisting of many facets, and changed their slopes according to Gaussian distribution with respect to surface wind. The computed emissivity in 11  $\mu\text{m}$  was 0.992 under no wind. Each of these studies in trying to determine the value of emissivity, failed to distinguish surface emission from reflection and to evaluate the temperature difference across the cool skin. The summary of these studies are tabulated in Table 1.

In this study, we directly measured the net infrared radiation near the sea surface, the upward radiation from the surface, and the temperature profile near the surface in order to determine the emissivity from the sea surface's radiation balance. The object of this paper is to determine the sea surface emissivity on the basis of meteorological and oceanographical observations throughout one year.

## 2. Emissivity

Radiation from the sea surface in the atmospheric window region, ranging  $\nu_1$  to  $\nu_2$ , is given by  $\bar{\epsilon} \int_{\nu_1}^{\nu_2} B(\nu, T_s) d\nu$  ( $\text{W} / \text{m}^2$ ), where  $B(\nu, T)$  is Planck function and  $\bar{\epsilon}$  is the surface emissivity averaged in the window region, and  $T_s$  is the skin temperature. If  $\bar{\epsilon} \neq 1$ , i.e., the sea water is not blackbody in the window region, atmospheric downward longwave radiation  $R_{\downarrow}$ , which comes

mainly from water vapor in the atmosphere, reflects at the sea surface. Therefore, the upward irradiance into the bottom of the atmosphere from the sea surface is the sum of the surface irradiance and the reflection at the surface; i.e.

$$\int_{\nu_1}^{\nu_2} B(\nu, T_R) d\nu = \bar{\epsilon} \int_{\nu_1}^{\nu_2} B(\nu, T_S) d\nu + (1 - \bar{\epsilon}) R\downarrow. \quad (1)$$

Here, we assume that the reflectance  $\gamma$  is equal to  $1 - \bar{\epsilon}$ .  $T_R$  is the radiometer temperature corresponding to the upward irradiance into the infrared radiometer near the sea surface. This radiation balance holds in the atmospheric window region.

When  $T_R$  is nearly equal to  $T_S$ , the difference between  $\partial B(\nu, T_R)/\partial \nu$  and  $\partial B(\nu, T_S)/\partial \nu$  is sufficiently small to neglect (McMillin, 1975). Therefore, the dependence on the wavenumber of  $B(\nu, T_S)$  is almost the same as that of  $B(\nu, T_R)$  and Eq. (1) can be expanded over all wavelength to be rewritten

$$\sigma T_R^4 = \bar{\epsilon} \sigma T_S^4 + (1 - \bar{\epsilon}) R\downarrow. \quad (2)$$

Here,  $\sigma$  is the Stefan-Boltzman constant. Equation (2) is the simpler infrared radiation balance near the sea surface.

Note that  $T_R$  is different from skin temperature  $T_S$  and that the change in downward radiation from the atmosphere  $R\downarrow$  causes the upward irradiance into the bottom of the atmosphere ( $T_R$ ) to change, even for the same  $T_S$ .

The net radiation  $R_{\text{net}}$  is the difference between  $\sigma T_R^4$  and  $R\downarrow$ ,

$$R_{\text{net}} = \sigma T_R^4 - R\downarrow. \quad (3)$$

If  $R_{\text{net}}$  is directly measured by the net radiometer, the emissivity can be evaluated by Eq. (4),

$$\bar{\epsilon} = \frac{R_{\text{net}}}{\sigma T_S^4 - \sigma T_R^4 + R_{\text{net}}}. \quad (4)$$

If the skin temperature  $T_S$  equals the water temperature near the surface as measured by a thermometer; i.e.,

$$T_S = T_B, \quad (5)$$

we can evaluate the calculated emissivity  $\bar{\epsilon}_C$  by using the measured variables, i.e.

$$\bar{\epsilon}_C = \frac{R_{\text{net}}}{\sigma T_B^4 - \sigma T_R^4 + R_{\text{net}}}. \quad (6)$$

Equation (5) means that temperature difference,  $\Delta T \equiv T_B - T_S$ , vanishes; i.e., the skin layer is disturbed.

### 3. Observation

To determine the value of emissivity, upward and net infrared radiation and other oceanographic and meteorological variables were measured at the oceanographic observatory tower of Kyoto University in Tanabe bay, Japan. Figure 1 shows the location of the tower, which is located on a ridge at a mean depth of about 5 m, and about 100 m from the shore. The observation was carried out from November 1989 to October 1990, with occasional interruption by meteorological disturbances such as typhoons. The number of days when available data were taken is tabulated on Table 2.

Figure 2 illustrates the arrangement of the equipment. Measured data were recorded every 10 minutes. Upward infrared radiation from the sea surface was measured by the *Minolta IR-0510* infrared radiometer (A), which was mounted about 5 m above the mean sea surface. Its viewing solid angle was  $1^\circ$ , and the sensitive wave length range was between  $8 \mu\text{m}$  and  $14 \mu\text{m}$ . We used

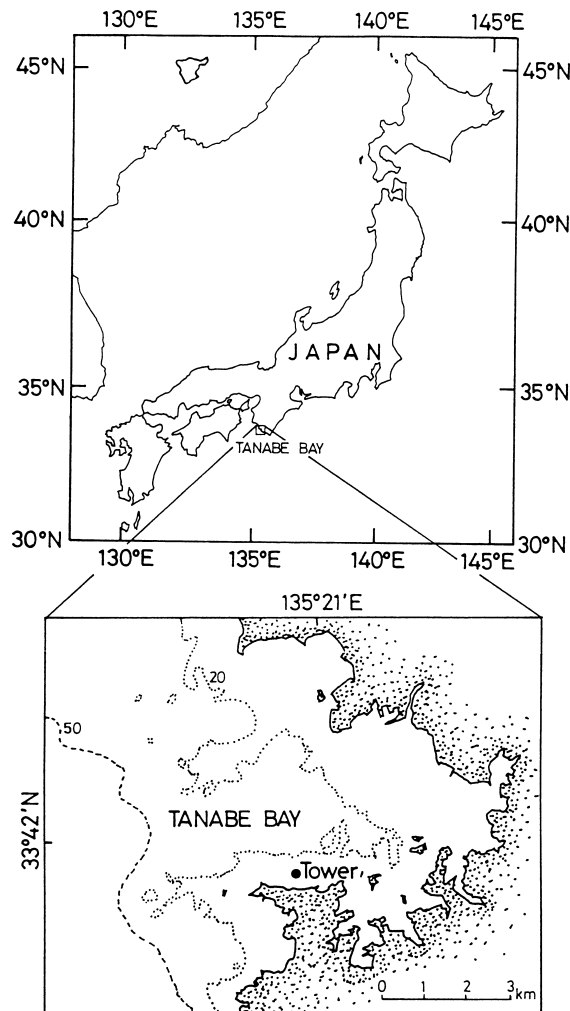


Fig. 1. Location of Shirahama and Oceanographic observatory tower. The tower is shown as a solid circle.

Table 2. The number of data available for the analyses, and data which is not available due to weather conditions and insufficient equipment.

Year month	Days with available data	Days with unavailable data	Days with no data
1989 Nov.	15	0	15
Dec.	7	1	23
1990 Jan.	5	9	17
Feb.	0	4	24
Mar.	3	5	23
Apr.	21	9	0
May	17	14	0
Jun.	8	11	11
Jul.	0	0	31
Aug.	10	5	16
Sep.	10	8	12
Total	96	67	182

the average of 5 data, which were taken at 2 second intervals. Net infrared radiation was measured by the *Eiko Seiki CN-40* net radiometer (B) mounted about 5 m above the mean sea surface. As its wave length range was over  $0.2 \mu\text{m}$ , the output was contaminated by solar insolation during daytime. At night, on the other hand, accuracy of the net infrared radiation was about 5% of its measured signal. Therefore, we used data measured at night. Relative humidity was also measured by the dry and wet bulb thermometer (F) about 5 m above the mean sea surface. As these sensors were sheltered from the sun, dry temperature was regarded as air temperature at about 5 m. Wind speed was taken from 1 minute averages at a height of 10 m above the mean sea level (G).

SST and air temperature were measured by the electric resistance thermistor thermometer whose time constant was 7.5 s and assumed error was  $0.1^\circ\text{C}$ . The vertical profiles of water and air temperature the near sea surface were measured by these sensors moored to buoy D in Fig. 2. Fifteen water temperature sensors, D1~D15, were set up on this buoy. The center of D1 (top sensor) was at a 0.7 cm depth from the plain sea surface without waves. This buoy was small and followed the sea surface fluctuations very well. Sensors from D1 to D9 were set at 1-cm intervals and from D10 to D15 at 2-cm intervals. Six sensors for air temperature near the sea surface were also set on this buoy (C) at heights of 10 cm, 20 cm, 40 cm, 80 cm, 120 cm and 160 cm. Another buoy (E) moored the thermistor thermometer chain, which had 15 sensors named E1~E15 from the top at 25-cm intervals. Air and sea surface temperatures at each depth were measured every 10 minutes. Typical time series records of the variables from 19th to 21th November, 1989 are shown as an example in Fig. 3. Small perturbations in the data are removed by the running mean procedure for 170 minutes. Because the output of the net radiometer is greatly effected by solar insolation (shaded areas in Fig. 3(b)), only night time data (20:00~3:50) are available for the analysis of infrared radiation balance.

As shown in Fig. 3(b), in most cases, the changes in net radiation during the night are very small except in bad weather. Figure 3(a) shows that the radiometer temperature ( $T_R$ ), assuming the emissivity as 1.00, is different from the bulk sea surface temperature ( $T_B$ ).

Due to its extreme thinness, it is impossible to directly measure the temperature difference

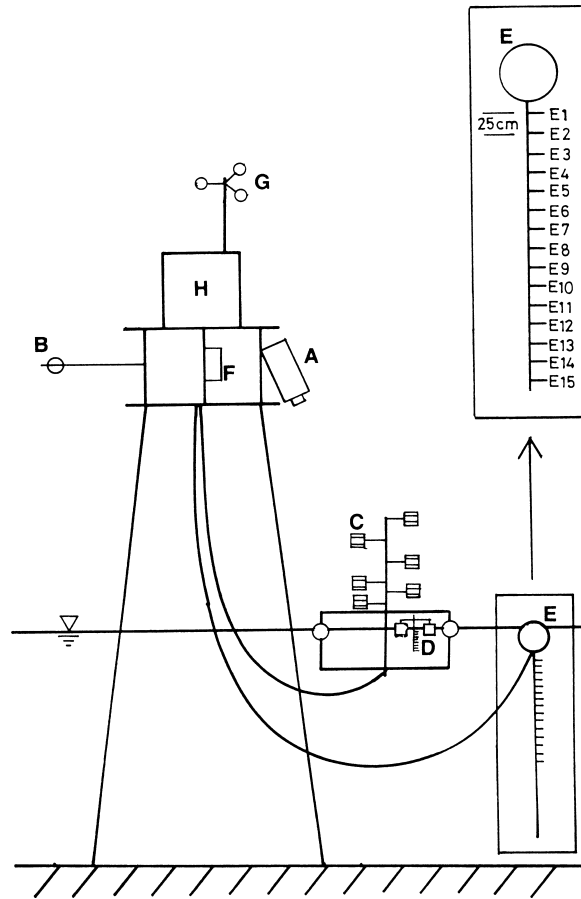


Fig. 2. Instruments set on the platform. A: Infrared radiometer. B: Infrared net radiometer. C: Thermistor thermometers for air temperature, C1~C6 from the top. D: Thermistor thermometers for near surface temperature, D1~D15 from the top, D1 to D9 are at 1-cm intervals and D10 to D15 are at 2-cm intervals. D1 is almost 1 cm from the surface. D15 is about 20 cm from the surface. E: Thermistor thermometers for water temperature, E1~E15 from the top, which are at 25-cm intervals. F: Dry and wet bulb psychrometer. G: Anemometer. H: Cabin.

across the skin layer using an ordinal method of oceanographic observation (Woodcock, 1941; Hasse, 1963; McAlister and McLeish, 1969; Paulson and Simpson, 1981; etc.). The skin layer is thought to be effected by meteorological and oceanographic conditions near the sea surface.

Katsaros (1980) reported that the skin layer changes its thickness due to  $\Delta T$  because the layer is formed by thermal conductivity. Field observations, however, are too rare to determine the thickness of the skin layer. We measured the vertical temperature profile of the sea surface at 1-cm intervals. Figure 4 shows the time variation of vertical profiles of water temperature on (a) November 19th (average wind speed was 10.2 m/s), and (b) June 11th (average wind speed was 0.6 m/s). No evidence is shown in Fig. 4 that the cool skin exists on the sea surface. The nearly constant vertical temperature profile allows us to consider the top sensor temperature as a subsurface temperature below the skin layer, and we confirm the skin layer is thinner than 1 cm if it exists in both cases.

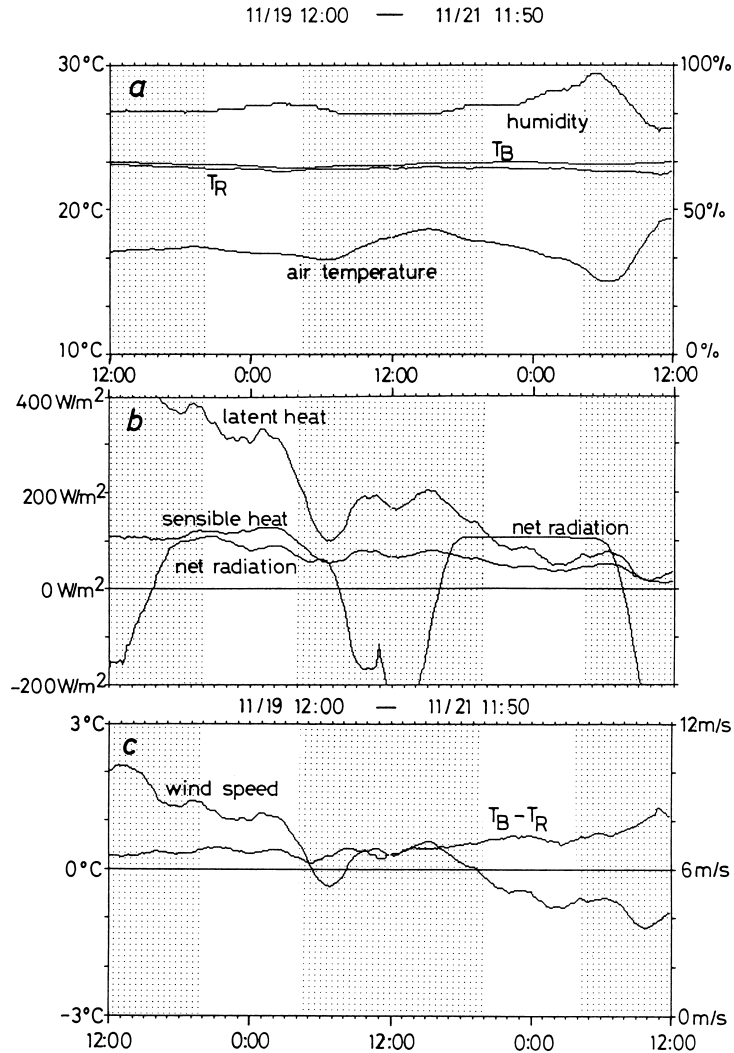


Fig. 3. Time series records of (a) the air temperature, the bulk temperature ( $T_B$ ), the radometer temperature ( $T_R$ ), and the relative humidity, (b) the heat fluxes, (c) wind speed and the temperature difference between  $T_R$  and  $T_B$ . Data in the shaded area is not used for the analyses because of disturbances by solar insolation.

Validity of  $\overline{\varepsilon_C}$  depends on whether Eq. (5) is correct or not. Water near the surface might be well mixed due to strong wind stress under high wind speed. Equations (1) and (2) show that skin temperature  $T_s$  effects radiometer temperature  $T_R$ . The time series record of the difference,  $T_B - T_R$ , is shown in Fig. 3(c).  $T_B - T_R$  is not the temperature difference,  $\Delta T$ , across the cool skin. When net radiation shows little time variation at night as in Fig. 3(b), the changes in  $T_R$  can be attributed to those in  $T_s$ , i.e., most of the changes in  $T_B - T_R$  can be regarded as  $\Delta T$ . The inverse correlation between wind speed variation and  $T_B - T_R$  variation suggests mixing by wind stress.

Figure 5 shows the relation between  $\overline{\varepsilon_C}$  averaged from 20:00 to 3:50 and mean wind speed. Unreliable values such as those caused by rainfall, wind bursts, and damage to the equipment are

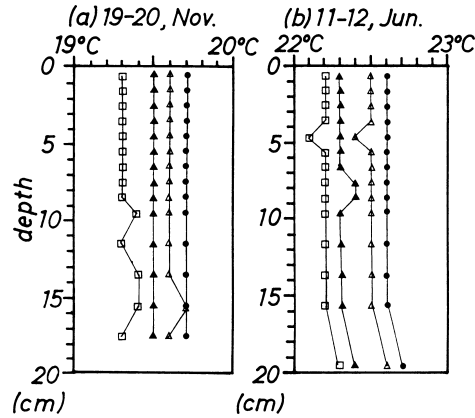


Fig. 4. Time variations in 2 hour averaged temperature profiles of the sea surface in (a) 19th~20th November, and (b) 11th~12th June. Each profile is averaged over 2 hours; ● 20:00~21:50, △ 22:00~23:50, ▲ 0:00~1:50, □ 2:00~3:50. Assumed error is 0.1°C.

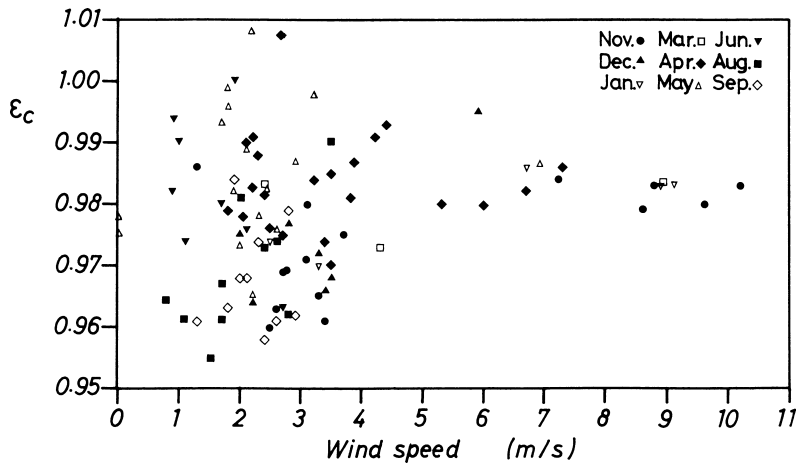


Fig. 5. Apparent dependence of  $\overline{\varepsilon_C}$  from Eq. (6) on wind speed. The emissivity and wind speed are averaged during 20:00~3:50.

deleted. The values of  $\overline{\varepsilon_C}$  distribute between 0.96 and 1.01, and have no correlation with wind speed in low winds. On the other hand, under conditions where wind speed exceeds 5 m/s,  $\overline{\varepsilon_C}$  shows a constant of  $0.984 \pm 0.004$ . Figure 5 shows this value does not change seasonally. Because the emissivity should be a physical constant, this value should be valid at lower wind speeds. The appropriate speculation for this constant temperature difference should be that the surface mixing due to the high wind stress cause to Eq. (5) to hold. It is said that the vertical velocity near the surface increases above a wind speed of about 5 m/s (Csanady, 1990; Ebuchi *et al.*, 1993), and the disappearance of the cool skin can be attributed to this vertical velocity.

Data obtained during rain, wind bursts, and other hard conditions are not available. Figure 6 shows two examples of the time change of  $\overline{\varepsilon_C}$  from 20:00 to 3:50; one is under clear weather conditions (25th~26th, March: dashed line) and the other is under the rainy conditions (3rd~4th,

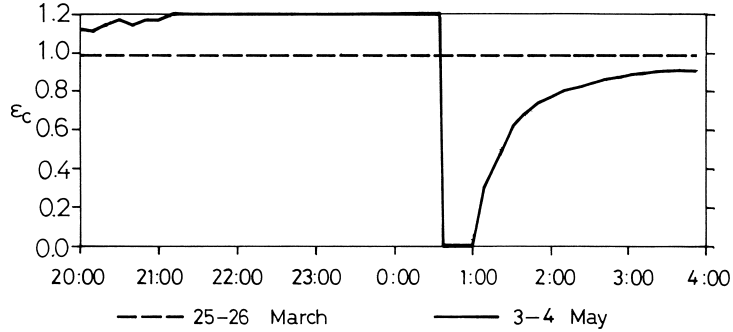


Fig. 6. Time series records of the computed emissivity  $\overline{\varepsilon_C}$ . Hard line: The computed emissivity on May 3rd. Dashed line: The computed emissivity on March 25th with calm weather.

May: solid line). The dashed line shows the small time variation with a standard deviation of 0.003. It is found that the time variation of  $\overline{\varepsilon_C}$  tends to be small under calm weather. The solid line, on the other hand, shows a sharp change at midnight: apparently, raindrops falling on the upper optical filter caused the downward radiation signal from the radiometer to increase.

#### 4. Discussion and Conclusions

Figure 5 shows that the surface skin layer can exist under low wind and disappear under high wind, and also shows that the value of emissivity is  $0.984 \pm 0.004$ . Comparing this value with previous studies, that of Buettner and Kern (1965) ( $\bar{\varepsilon} = 0.993$ ) is larger. Saunders' emissivity value (1967b, 1968) ( $\bar{\varepsilon} = 0.986$ ) agrees well with ours. In Saunders' experiment using an airborne radiometer, the horizontal variation of the sky, cloud and sea surface temperature was occasionally small and the reflection was successfully separated from the surface irradiance. The result of Davies *et al.* (1971) was  $\bar{\varepsilon} = 0.972 \pm 0.021$ . In their experiment,  $T_R$  and  $T_S$  were measured by an infrared radiometer.  $T_S$  was measured by isolating the sea surface from sky radiation by placing an aluminum cone over the water. Because the cone rim was under water, surface mixing was suppressed compared to the  $T_R$  measurement. Judging from the method of their experiment and the larger standard deviation in the result, their data should correspond to the low wind regime in our experiment.

Variation of  $\overline{\varepsilon_C}$  at low wind speed (Fig. 5) is caused by the temperature difference between the cool skin and the subsurface; i.e., the surface skin layer is not disturbed by weak wind speeds, and the relation (5) does not hold under this condition. When  $T_S$  is higher than  $T_B$ , a higher value of  $\overline{\varepsilon_C}$  is computed than the true value of  $\bar{\varepsilon}$ , and a lower value is obtained when  $T_S$  is lower than  $T_B$ .

Contrary to our hypothesis that the skin layer can vanish at high wind speeds, the previous studies (Saunders, 1967a; Hasse, 1971; Grassl, 1976; Wesely, 1979; etc.) considered that the temperature difference does not vanish. Therefore, we need to examine whether  $\Delta T$  vanishes at high wind speed.

Saunders (1967a) discussed the value of  $\Delta T$ , assuming that cool skin is not disturbed by wind. Later studies of the cool skin focused on determining  $\Delta T$  observationally based on Saunders' idea. The temperature difference across the cool skin  $\Delta T$  was determined as the difference between the skin and subsurface temperatures.

Hasse (1971) determined  $T_S$  from the air temperature profile, assuming a diabatic and near

neutral condition; i.e., he took an indirect method to determine  $T_S$ . He reported that the averaged value of  $\Delta T$  was  $0.4^\circ\text{C}$ . Using a thermometer and radiometer, Grassl (1976) determined  $\Delta T$  as the difference between the subsurface temperature at a depth of 5 cm and the temperature corresponding to the radiance into the bottom of the atmosphere. In his study,  $\Delta T$  was almost constant at  $0.2^\circ\text{C}$  for a wind speed of 1 to 10 m/s. He estimated the skin temperature, assuming the surface emissivity to be 0.96 in advance. Wesely (1979) reported that  $\Delta T$  varied from  $0.3^\circ\text{C}$  to  $1.5^\circ\text{C}$ , but he assumed the emissivity to be 0.99 and did not consider surface reflection. In the studies of both Grassl (1976) and Wesely (1979), the basis for determining the value of emissivity was not clear. In fact, their results on the temperature difference  $\Delta T$  depended on an arbitrarily determined value of emissivity. For example, applying  $\bar{\epsilon} = 0.984$  to Grassl's data instead of his value  $\bar{\epsilon} = 0.96$ , we found that  $\Delta T$  becomes almost  $0^\circ\text{C}$ . Therefore, although their result showed that  $\Delta T$  does not become  $0^\circ\text{C}$ , it is clearly possible for  $\Delta T$  to vanish under high wind speeds.

Now, we will examine if the assumption  $T_S = T_B$  really holds under high wind speeds when we adopt the present result ( $\bar{\epsilon} = 0.984$ ). We computed the temperature difference  $\Delta T$  in order to test the wind speed's influence on the change of the surface layer. By adopting the present result ( $\bar{\epsilon} = 0.984$ ),  $T_S$  is given by Eq. (7),

$$T_S = \left( \frac{\bar{\epsilon}\sigma T_R^4 + (1 - \bar{\epsilon})R_{\text{net}}}{\bar{\epsilon}\sigma} \right)^{1/4}, \quad (7)$$

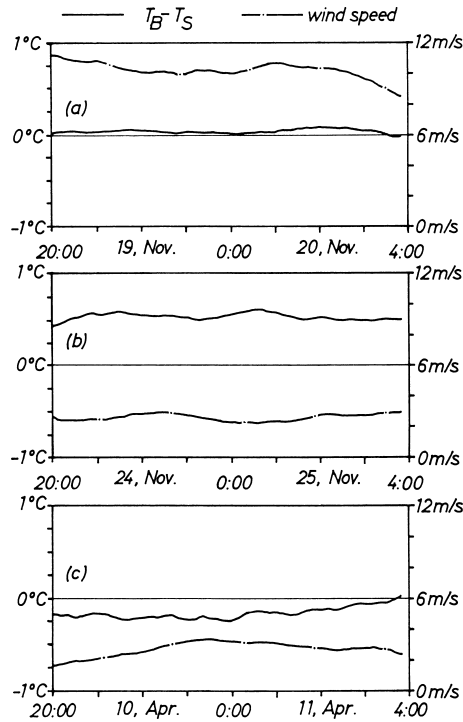


Fig. 7. Time changes of the temperature difference  $\Delta T$  and the wind speed on (a) November 19th, (b) April 10th and (c) November 24th.

and  $T_B$  is measured by the sensor D1. Time change for the temperature difference  $\Delta T (=T_B - T_S)$  is shown in Fig. 7 for 3 types (panels (a), (b) and (c)) of typical skin layer conditions. The panel (a) is on November 19th, when wind speed is large (averaged wind speed is 10.2 m/s). The temperature difference  $\Delta T$  disappears as we speculated; i.e., the surface skin layer is well mixed under large wind stress. Panel (b) in Fig. 7 shows the time change on November 24th, when the wind speed was weak (averaged wind speed was 2.6 m/s) and the calculated emissivity  $\overline{\epsilon_C}$  was less than 0.984. Panel (b) shows that  $T_S$  was lower than  $T_B$  under this condition and that the cool skin exists in the upper thin layer above the sensor D1. Panel (c), on the other hand, shows the time change on April 10th, when the wind was weak (averaged wind speed was 2.6 m/s) and  $\overline{\epsilon_C} > 0.984$ .  $T_S$  is higher than  $T_B$  under this condition, meaning the surface skin layer can be warmer than the subsurface.

Although Saunders (1967a) considered that the surface skin layer always exists, these results support our speculation that the warm and cool skin layers exist under weak wind stress due to the thermal conditions near the sea surface and can be disturbed and destroyed by strong wind stress. In the case of warm skin, the surface temperature  $T_S$  is higher than the subsurface temperature  $T_B$  and the calculated emissivity  $\overline{\epsilon_C}$  is larger than 0.984. To examine when the three types of skin layers tend to appear, the monthly variation is shown in Fig. 8 (panel (d)); where the white block shows surface skin cooler than the subsurface ( $\overline{\epsilon_C} < 0.980$ ), the stripe block shows surface temperature close to the subsurface temperature ( $0.980 \leq \overline{\epsilon_C} \leq 0.988$ ), and the slant line block shows surface skin layer warmer than the subsurface ( $\overline{\epsilon_C} > 0.988$ ). In Fig. 8, the monthly mean

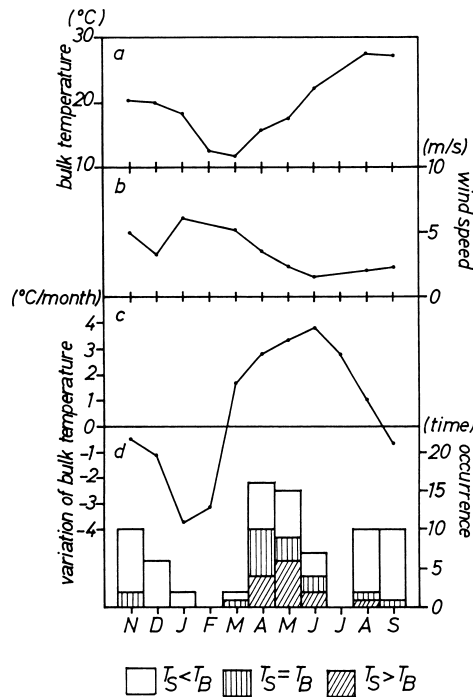


Fig. 8. Monthly means of (a) bulk sea surface temperature, (b) wind speed and (c) time change of panel (a). The histogram of the value of  $\overline{\epsilon_C}$  is (d).

of the subsurface temperature  $T_{B100}$  at a 1 m depth (panel (a)), that of the wind speed (panel (b)), and the time change of the monthly mean subsurface temperature (panel (c)) are correlated with each other because, in winter, strong seasonal wind blows during fine weather, but in summer, fine weather is usually accompanied by light wind. Figure 8 shows that the cool surface skin appears throughout the year. Comparing panel (d) with panel (c), cases where the cool skin is absent are well correlated with the time change of the bulk water temperature; i.e., the warm surface skin layer appears frequently when the bulk sea surface temperature increases and the subsurface boundary layer warms. Moreover, the surface layer is neutral even under low wind speed as conditions change from warm to cool and vice versa. The zero occurrence in February and July means “no data” because of trouble with the measuring system.

Standard deviation of the reliable value (at a wind speed over 5 m/s) of the computed emissivity is 0.004. This should be due to observational error. For example, consider that  $R\uparrow = 387.1 \text{ W/m}^2$ ,  $R_{\text{net}} = 125.2 \text{ W/m}^2$ , and  $T_B = 14.6^\circ\text{C}$ , which are the averaged values from 20:00 on 25th to 3:50 on 26th in March, and the change of  $0.1^\circ\text{C}$  in  $T_B$ , which is the accuracy of the thermister thermometer, produce the change of 0.004 in the emissivity derived from Eq. (6). This is equivalent to the standard deviation of our result. In addition, the 5% change in  $R_{\text{net}}$ , the accuracy of the net radiometer, produces a small change of 0.0006 in the emissivity.

Water temperature obtained from satellite observations is the skin layer temperature, whereas SST from oceanographic observations usually refers to the subsurface water at a depth ranging from several dozen centimeters to several meters. Traditionally, SST retrieved from satellite infrared observation has been defined as the surface blackbody temperature. The difference between these temperatures would be reduced by considering the sea surface as a graybody. Saunders (1970) expressed the improvement as a temperature, ranging from  $0.1^\circ\text{C}$  to  $0.7^\circ\text{C}$  depending on cloud types. We examined the reduction in temperature difference with a rate of error reduction. In this study, we define the temperature difference between the radiation temperature  $T_R$  and the temperature  $T_{B50}$  at a depth of 50 cm (sensor E2) where bucket water is sampled in standard oceanographic observations as

$$\Delta T_R = T_{B50} - T_R. \quad (8)$$

The rate of error reduction  $E$  is defined by Eq. (9) as the ratio of the improvement using this result over the previous temperature difference assuming blackbody, and shows what percentage of  $\Delta T_R$  is reduced when an emissivity value of 0.984 is adopted, i.e.,

$$\begin{aligned} E &= \frac{(T_{B50} - T_R) - (T_{B50} - T_S)}{T_{B50} - T_R} \\ &= \frac{T_S - T_R}{\Delta T_R}. \end{aligned} \quad (9)$$

Figure 9 shows the histogram of rate  $E$  evaluated from the 96 available night time data. Figure 9 shows that 40~60% of the temperature difference is reduced by taking the emissivity as 0.984 rather than 1.00. In Fig. 9, negative value of  $E$  means that temperature difference increases. This case occurs when both skin temperature  $T_S$  and radiation temperature  $T_R$  are higher than the bucket temperature.

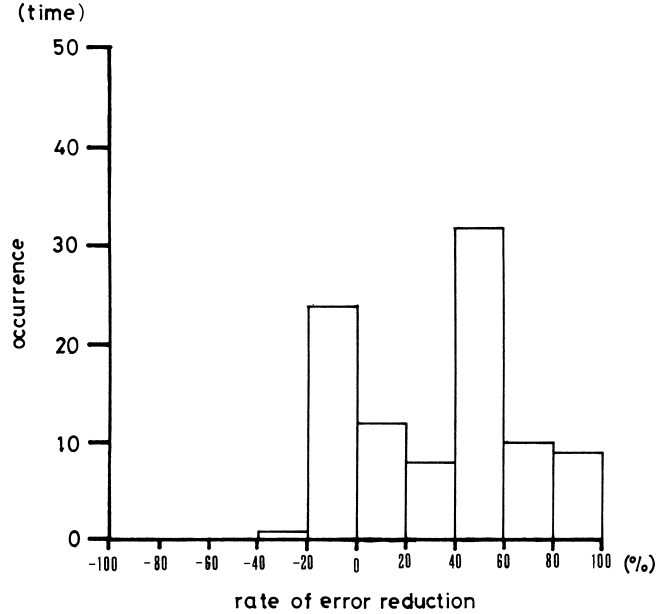


Fig. 9. Rates of improvements in temperature difference between  $T_R$  and  $T_{B50}$ . Determination of the emissivity as 0.984 leads to a reduction in the temperature difference. In many cases, 40~60% of the temperature difference is reduced.

In the analyses of the satellite infrared data, the reflection at the sea surface has been ordinarily neglected (i.e.,  $R\downarrow$  in Eq. (7) is neglected), even though the sea surface has been considered as a graybody, and the SST has been evaluated by Eq. (10),

$$T_S = \left( \frac{T_R^4}{\bar{\epsilon}} \right)^{1/4}. \quad (10)$$

We examined the difference between the temperature obtained from Eq. (7) and that obtained from Eq. (10), and found that the difference of about  $0.8^\circ\text{C}$  is produced for the data on May 26th when  $T_S$  is  $14.7^\circ\text{C}$  from Eq. (7) and  $15.5^\circ\text{C}$  from Eq. (10). This result and the tests using other data show that  $R\downarrow$  in Eq. (7) cannot be neglected in computing  $T_S$ .

It is known that the emissivity changes with the electric conductivity, i.e., the salinity of sea water. Liu *et al.* (1987) asserted that salinity variations effect the value of emissivity. On the other hand, the experiment of Davies *et al.* (1971) showed that chemical characteristics have little effect on the value of emissivity. This problem must be addressed in the future.

Our conclusions are as follows;

- 1) We performed oceanographic and meteorological observations for one year at the tower station in Tanabe bay, Japan, and found that the reliable value of emissivity is  $\bar{\epsilon} = 0.984 \pm 0.004$ .
- 2) Adopting our result ( $\bar{\epsilon} = 0.984$ ) reduces in half the temperature difference between the bucket temperature and the radiometer temperature by assuming the sea surface to be a blackbody. Additionally, we found that we could not neglect the surface reflection of the atmospheric downward radiation in the temperature retrieval for the satellite infrared data.

3) We found that the skin layer at the sea surface disappears under wind speeds larger than 5 m/s due to wind stress disturbances, adopting the present result as the emissivity.

4) The surface skin layer changes from warm to cool due to thermal conditions under low wind speeds. The cool skin layer appears throughout the year, and the warm skin layer is produced from April to June when the subsurface temperature warms and the wind stress weakens. The skin layer can be thermally neutral even under low wind speed as conditions change from warm to cool and vice versa.

### Acknowledgements

We gratefully acknowledge the cooperation of the members of Shirahama Oceanographic Observatory of Disaster Prevention Research Institute at Kyoto University in taking data and maintaining the instruments. We are also grateful for the support and advice of Professor Takagi of the University of Tokyo. Part of this study was supported by the Grants-in-Aid for Scientific Research by the Ministry of Education, Science and Culture (No. 01646010).

### References

- Buettner, K. J. K. and C. D. Kern (1965): The determination of infrared emissivities of terrestrial surfaces. *J. Geophys. Res.*, **70**, 1329–1337.
- Csanady, G. T. (1990): The role of breaking wavelets in air-sea gas transfer. *J. Geophys. Res.*, **95**, 749–759.
- Davies, J. A., P. J. Robinson and M. Nunez (1971): Field determination of surface emissivity and temperature for Lake Ontario. *J. Appl. Meteor.*, **10**, 811–819.
- Ebuchi, N., H. Kawamura and Y. Toba (1993): Bursting phenomena in the turbulent boundary layer beneath the laboratory wind-wave surface. p. 263–276. In *Natural Physical Sources of Underwater Sound*, ed. by B. R. Kerman, Kluwer Academic Publisher.
- Grassl, H. (1976): The dependence of the measured cool skin of the ocean on wind stress and total heat flux. *Boundary-Layer Meteor.*, **10**, 465–474.
- Hasse, L. (1963): On the cooling of the sea surface by evaporation and heat exchange. *Tellus*, **15**, 363–366.
- Hasse, L. (1971): The sea surface temperature deviation and the heat flow at the sea-air interface. *Boundary-Layer Meteor.*, **1**, 368–379.
- Katsaros, K. B. (1980): The Aquaeous thermal boundary layer. *Boundary-Layer Meteorol.*, **18**, 107–127.
- Liu, W.-Y., R. T. Field, R. G. Gantt and V. Klemas (1987): Measurement of the surface emissivity of turbid waters. *Remote Sens. Environ.*, **21**, 97–109.
- Masuda, K., T. Takashima and Y. Takayama (1988): Emissivity of pure and sea waters for the model sea surface in the infrared window regions. *Remote Sens. Environ.*, **24**, 313–329.
- McAlister, E. D. and W. McLeish (1969): Heat transfer in the top millimeter of the ocean. *J. Geophys. Res.*, **74**, 3408–3414.
- McMillin, L. M. (1975): Estimation of sea surface temperatures from two infrared window measurements with different absorption. *J. Geophys. Res.*, **80**, 5113–5117.
- Mikhaylov, B. A. and V. M. Zolotarev (1970): Emissivity of liquid water. *Atmos. Oceanic Phys.*, **6**, 52.
- Paulson, C. A. and J. J. Simpson (1981): The temperature difference across the cool skin of the ocean. *J. Geophys. Res.*, **86**, 11044–11054.
- Saunders, P. M. (1967a): The temperature at the ocean-air interface. *J. Atmos. Sci.*, **24**, 269–273.
- Saunders, P. M. (1967b): Aerial measurement of the sea surface temperature in the infrared. *J. Geophys. Res.*, **72**, 4109–4117.
- Saunders, P. M. (1968): Radiance at sea and sky in the infrared window 800–1200  $\text{cm}^{-1}$ . *J. Opt. Soc. Amer.*, **58**, 645–652.
- Saunders, P. M. (1970): Corrections for airborne radiation thermometry. *J. Geophys. Res.*, **36**, 7596–7601.
- Schluessel, P., W. J. Emery, H. Grassl and T. Mammen (1990): On the bulk-skin temperature difference and its impact on satellite remote sensing of sea surface temperature. *J. Geophys. Res.*, **95**, 13341–13356.
- Wesely, M. L. (1979): Heat transfer through the thermal skin of a cooling pond with waves. *J. Geophys. Res.*, **84**, 3696–3700.
- Woodcock, A. H. (1941): Surface cooling and streaming in shallow fresh and salt waters. *J. Mar. Res.*, **4**, 153–161.